Stars and their variability observed from space
C. Neiner, W. W. Weiss, D. Baade, R. E. Griffin, C. C. Lovekin, A. F. J. Moffat (eds)

PROTOSTELLAR ACCRETION BURSTS AND THEIR EFFECT ON PRE-MAIN-SEQUENCE STELLAR EVOLUTION

E. Vorobyov[1, 2] and V. Elbakyan[2]

Abstract. The pre-main-sequence evolution of low-mass stars and brown dwarfs has been studied numerically by considering the accretion of mass onto the central object. Stellar evolution was computed using the STELLAR evolution code developed by Yorke & Bodenheimer. Mass accretion rates were taken from numerical hydrodynamics models of Vorobyov & Basu. We found that mass accretion can have a strong effect on the subsequent evolution of young stars and brown dwarfs. Accreting and non-accreting models disagree with each other, and the extent of the disagreement depends notably on the thermal efficiency of accretion. The largest mismatch is found for the cold accretion case. In the hot and hybrid accretion cases the disagreement between accreting and non-accreting models is less pronounced, but still remains noticeable for 1.0 M-yr-old objects. A wrong age estimate for objects of (sub-)solar mass is possible if isochrones based on non-accreting models are used.

Keywords: accretion, stars: formation, low-mass, brown dwarfs, pre-main sequence

1 Introduction

The evolution of pre-main-sequence (PMS) stars has been studied for decades by various authors (e.g., Baraffe et al. 1998; Palla & Stahler 2000), but only recently has it become possible to study stellar evolution starting from the very early stages of star formation and taking the main accretion phase into account. Solar-type stars form through gravitational collapse of molecular cloud cores, and circumstellar disks form because of the near-conservation of the angular momentum in the collapsing cores. In the early embedded phase of protostellar disk evolution the disks are often prone to gravitational instability (Vorobyov & Basu 2009), which results in very time-dependent mass accretion histories, the episodic accretion histories repeating short accretion bursts and relatively longer quiescent phases (Vorobyov & Basu 2010, 2015; Machida et al. 2011). Other mechanisms, such as the magneto-rotational and thermal instabilities, planet-disk interactions and close stellar encounters, can also produce episodic accretion bursts in both the embedded and T Tauri phases of disk evolution (see Audard et al. (2014) for a review). Various observational signatures of this episodic accretion have also been reported for low-mass protostars (e.g., Dunham et al. 2010; Liu et al. 2016). The effects of such variable mass accretion have recently been included in the stellar evolution calculations focussing on the early (Vorobyov 2016) and late stellar evolutionary phases (e.g., Baraffe et al. 2009, 2012, 2017; Hosokawa et al. 2013).

Those studies revealed that the PMS tracks of accreting stars can differ from the non-accreting tracks that have routinely been used to estimate stellar ages and masses of young clusters. In particular, the age of a star as inferred from non-accreting tracks can be considerably overestimated. We show that the thermal efficiency of accretion, i.e., the fraction of accretion energy retained by the star (normally incorporated as a free parameter of the model), can affect the stellar evolution tracks of accreting stars appreciably. It is therefore still quantitatively uncertain to what extent non-accreting isochrones are reliable after all, and whether it is accretion variability or thermal efficiency of accretion that plays the main role in PMS evolution.

2 Numerical model

2.1 Hydrodynamics code

Mass accretion histories were computed using the numerical hydrodynamics models of star and disk evolution described in detail in Vorobyov & Basu (2010). We started our numerical simulations from the gravitational

[1] University of Vienna, Department of Astrophysics, Vienna 1180, Austria
[2] Research Institute of Physics, Southern Federal University, Stachki Ave. 194, Rostov-on-Don 344090, Russia

collapse of a gravitationally contracting cloud core, continued into the embedded phase of star formation during which star, disk and envelope are formed, and terminated our simulations after the point corresponding to 1.0–2.0 Myr of evolution, depending on the model and available computational resources. We assumed that in subsequent evolution the mass accretion rate declines linearly to zero during another 1.0 Myr. That effectively sets a disk dispersal time of 1 Myr and a total disk age of about 2.0–3.0 Myr in our models. Those values are in general agreement with the disk ages inferred from observations of star-forming regions (Williams & Cieza 2011).

2.2 Stellar evolution code

We computed the evolution of low-mass stars and higher-mass brown dwarfs using the evolution code STELLAR originally developed by Yorke & Bodenheimer (2008). We started our computations from a protostellar seed, continued through the main accretion phase where the growing star accumulates most of its final mass, and ended the computations when the star approached the main sequence. We used the protostellar accretion rates obtained from the numerical hydrodynamics simulations of pre-stellar core collapse described in Sect.2.1.

2.3 Thermal efficiency of accretion

During the evolution calculations we assumed that a fraction α of the accretion energy $\epsilon G M_* \dot{M}/(2R_*)$ is absorbed by the protostar, while a fraction $1-\alpha$ is radiated away and contributes to the accretion luminosity of the star. M_* and R_* are the mass and radius of the central star, and $\dot{M}$ is the mass accretion rate. Here we consider three models for the thermal efficiency of accretion: (i) cold accretion with a constant $\alpha = 10^{-3}$, meaning that practically all accretion energy is radiated away and little is absorbed by the star, (ii) hot accretion with a constant $\alpha = 0.1$, and (iii) a hybrid scheme defined as follows:

$$\alpha = \begin{cases} 10^{-3}, & \text{if } \dot{M} < 10^{-7}\ M_\odot\ \mathrm{yr}^{-1}\ , \\ \dot{M} \times 10^4 \left[\frac{\mathrm{yr}}{M_\odot}\right], & \text{if } 10^{-7}\ M_\odot\ \mathrm{yr}^{-1} \le \dot{M} \le 10^{-5}\ M_\odot\ \mathrm{yr}^{-1}, \\ 0.1, & \text{if } \dot{M} > 10^{-5}\ M_\odot\ \mathrm{yr}^{-1}. \end{cases} \quad (2.1)$$

3 Hybrid accretion

This section presents our results for the hybrid accretion model, in which the value of α depends on the mass accretion rate. The computed stellar evolution sequences of the total (accretion plus photospheric) luminosity L_* *vs.* effective temperature $T_{\rm eff}$ for 31 models are shown as the dots in the left panel of Fig. 1. The zero point of the stellar age (zero age) is defined as the instance when the growing star accumulates 95% of its final mass. The green symbols mark the reference ages of 1 Myr, 10 Myr, and 25 Myr for each model. The black solid lines present the isochrones for the same ages but derived from the non-accreting stellar evolution models of Yorke & Bodenheimer (2008) (hereafter, the non-accreting isochrones).

The left panel of Fig. 1 indicates that young 1-Myr-old stellar objects show a noticeable deviation from non-accreting isochrones of the same age. This is especially evident for models with effective temperatures of $\log T_{\rm eff} \ge 3.5$, which lie significantly lower than the 1.0-Myr-old isochrone, meaning that these objects appear older on the L_*–$T_{\rm eff}$ diagram than they truly are.

4 Hot accretion

This section discusses the results for the hot accretion model, in which α is set to 0.1 during the entire evolution period. For the models with the hot accretion scenario there again exists a moderate deviation between the accreting and non-accreting 1.0-Myr-old models as concerns the total luminosity and stellar radius, but this disagreement diminishes for 10-Myr-old and 25-Myr-old models. All in all, the behaviour of the hybrid and hot accretion models is similar, in agreement with the previous work of Baraffe et al. (2012).

5 Cold accretion

This section presents our results for the cold accretion model, in which α is always set to the small value of 10^{-3} independent of the actual value of the mass accretion rate, meaning that almost all accretion energy is radiated away and only a tiny fraction is absorbed by the protostar. The right panel of Fig. 1 shows the stellar

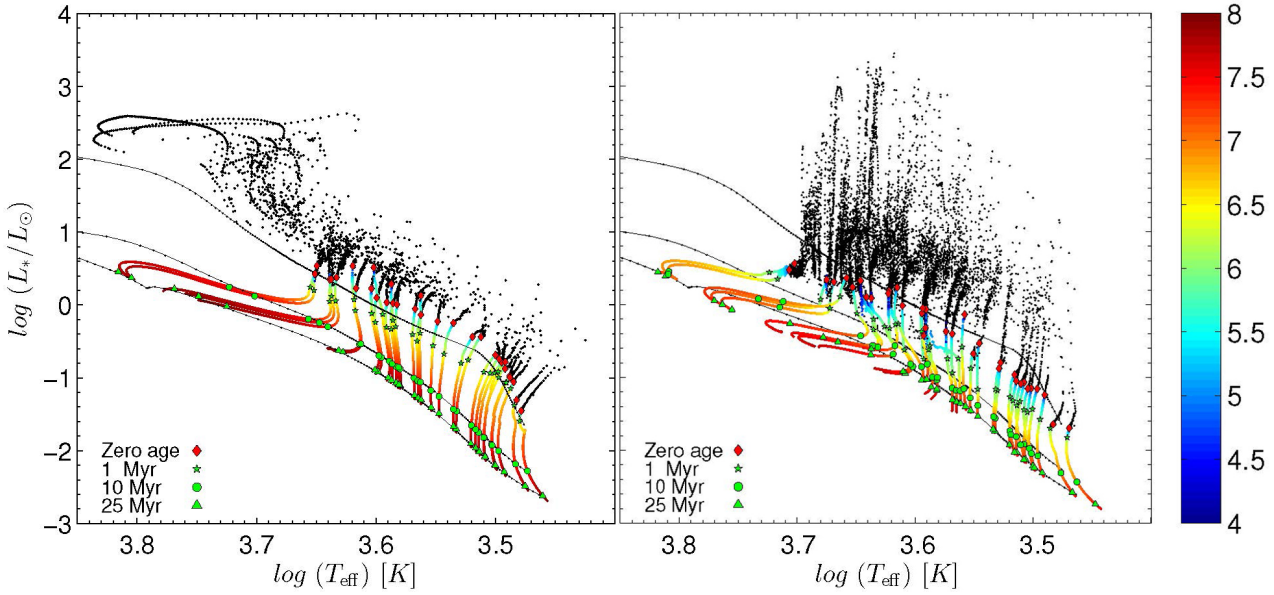

Fig. 1. Left: Stellar evolution sequences in the total luminosity L_* – effective temperature $T_{\rm eff}$ diagram for hybrid accretion models. The dots of various colours present the model tracks. The zero-point age for each model is marked by red diamonds. Green symbols mark the reference ages (as indicated in the bottom left corner) that have elapsed since the zero-point age of each object. The black solid lines indicate the isochrones for stellar ages of 1 Myr, 10 Myr and 25 Myr (from top to bottom) derived from the non-accreting stellar evolution models of Yorke & Bodenheimer (2008). **Right:** Similar to the left panel, but for the cold accretion model.

evolutionary sequences for all models. The meaning of the symbols and lines is the same as in the left panel of Fig. 1.

In general, the disagreement between the cold accretion models of a certain age and the corresponding non-accreting isochrones of Yorke & Bodenheimer has increased as compared to the case of hybrid (or hot) accretion. To quantify this disagreement, the red solid lines in Fig. 2 represent the non-accreting isochrones that best fit our 1 Myr-old stars. The resulting ages of these non-accreting isochrones are 1.5 Myr for hybrid accretion (top panel) and 4.5 Myr for cold accretion (bottom panel). The black lines show the non-accreting isochrones of 1 Myr age. This exercise demonstrates that 1-Myr-old accreting models can be fitted erroneously to 1.5-Myr-old or even 4.5-Myr-old non-accretion isochrones, meaning that the non-accreting isochrones can be unreliable for the stellar age estimates.

6 Conclusions

Our key findings can be summarized as follows:

- In the hybrid accretion case, young 1.0-Myr-old objects show substantial deviations from the non-accreting isochrones for both low-mass stars and brown dwarfs.
- The hot accretion case is qualitatively similar to hybrid accretion, but shows somewhat smaller deviations for L_* and R_*.
- The cold accretion case features the largest deviations from the non-accreting models of Yorke& Bodenheimer.
- As a result of this mismatch, the use of the L_*–$T_{\rm eff}$ diagram may lead to false age estimates for objects with $T_{\rm eff} > 3500$ K, as was also previously noted in Baraffe et al. (2009) and Hosokawa et al. (2011).

This project was supported by the Russian Ministry of Education and Science Grant 3.961.2014/K. The simulations were performed on the Vienna Scientific Cluster (VSC-2 and VSC-3) and on the Shared Hierarchical Academic Research Computing Network (SHARCNET).

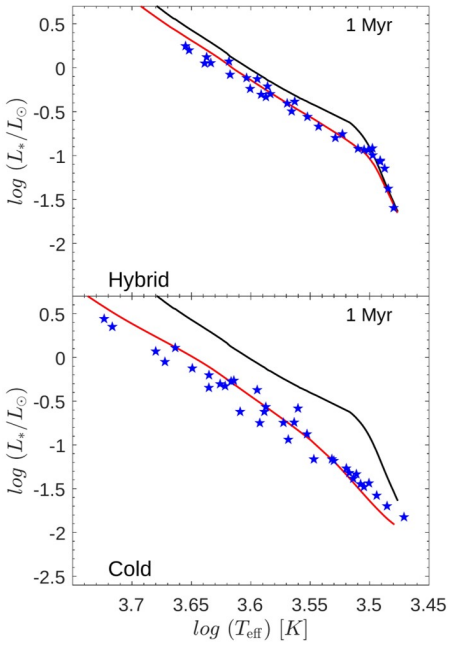

Fig. 2. Total luminosity–effective temperature diagram in the hybrid and cold accretion models. The star symbols represent our 1.0-Myr-old accreting models. The black solid lines are the isochrones (of the corresponding age) derived from the non-accreting models of Yorke & Bodenheimer (2008), while the red solid lines represent the non-accreting isochrones of Yorke & Bodenheimer that fit our model data best. The red solid lines represent the 1.5 Myr isochrone in the top panel and the 4.5 Myr isochrone in the bottom panel.

References

Audard, M., Ábrahám, P., Dunham, M. M., et al. 2014, in Protostars and Planets VI, ed. H. Beuther, R. S. Klessen, C. P. Dullemond, & T. Henning, 387

Baraffe, I., Chabrier, G., Allard, F., & Hauschildt, P. H. 1998, A&A, 337, 403

Baraffe, I., Chabrier, G., & Gallardo, J. 2009, ApJ, 702, L27

Baraffe, I., Elbakyan, V. G., Vorobyov, E. I., & Chabrier, G. 2017, A&A, 597, A19

Baraffe, I., Vorobyov, E., & Chabrier, G. 2012, ApJ, 756, 118

Dunham, M. M., Evans, II, N. J., Terebey, S., Dullemond, C. P., & Young, C. H. 2010, ApJ, 710, 470

Hosokawa, T., Offner, S. S. R., & Krumholz, M. R. 2011, ApJ, 738, 140

Hosokawa, T., Yorke, H. W., Inayoshi, K., Omukai, K., & Yoshida, N. 2013, ApJ, 778, 178

Liu, H. B., Takami, M., Kudo, T., et al. 2016, Science Advances, 2, e1500875

Machida, M. N., Inutsuka, S.-i., & Matsumoto, T. 2011, ApJ, 729, 42

Palla, F. & Stahler, S. W. 2000, ApJ, 540, 255

Vorobyov, E. I. 2016, A&A, 590, A115

Vorobyov, E. I. & Basu, S. 2009, MNRAS, 393, 822

Vorobyov, E. I. & Basu, S. 2010, ApJ, 719, 1896

Vorobyov, E. I. & Basu, S. 2015, ApJ, 805, 115

Williams, J. P. & Cieza, L. A. 2011, ARA&A, 49, 67

Yorke, H. W. & Bodenheimer, P. 2008, in ASPCS, Vol. 387, Massive Star Formation: Observations Confront Theory, ed. H. Beuther, H. Linz, & T. Henning, 189